High sodium reduced the expression of PTH1R and Klotho by inhibiting 1,25(OH)$_2$D$_3$ synthesis in cultured proximal tubule epithelial cells

Jie Gu[1,2#], Jialin Shi[1,2#], Xujiao Chen[1,2], Jianping Mao[1,2], Huaizhou You[1,2], Jing Chen[1,2]

[1]Division of Nephrology, Huashan Hospital, Fudan University, Shanghai, China; [2]National Clinical Research Center for Aging and Medicine, Huashan Hospital, Fudan University, Shanghai, China

Contributions: (I) Conception and design: J Chen; (II) Administrative support: J Chen; (III) Provision of study materials or patients: J Chen; (IV) Collection and assembly of data: J Gu, J Shi, X Chen, J Mao; (V) Data analysis and interpretation: J Gu, H You; (VI) Manuscript writing: All authors; (VII) Final approval of manuscript: All authors.

[#]These authors contributed equally to this work.

Correspondence to: Dr. Huaizhou You; Dr. Jing Chen. Division of Nephrology, National Clinical Research Center for Aging and Medicine, Huashan Hospital, Fudan University, Shanghai, China. Email: huaizhouyou@fudan.edu.cn; chenjing1998@fudan.edu.cn.

Background: The proximal tubule is the sensing site of sodium and phosphate and the main place for the synthesis and metabolism of 1,25(OH)$_2$D$_3$. We aimed to investigate the effects of high sodium on the synthesis and function of active vitamin D and local phosphate regulation in proximal tubular epithelial cells.

Methods: Human proximal tubule epithelial (HK-2) cells were treated with different concentrations of sodium/phosphate. The expression of 1α-OHase and 24-OHase was determined. Liquid chromatography/mass spectrometry (LC/MS) and enzyme-linked immunosorbent assay (ELISA) were used to detect the levels of 1,25(OH)$_2$D$_3$. RNA sequencing and bioinformatics analysis was used to probe into the possible pathways. Chromatin samples were immunoprecipitated with antibodies against parathyroid receptor 1 (PTH1R) and Klotho.

Results: We found that high sodium decreased the expression of 1,25(OH)$_2$D$_3$ by reducing 1α-OHase and 24-OHase, reduced the expression of PTH1R and Klotho, and increased the intracellular calcium concentration. These effects were reversed by sodium phosphate transporter inhibitor, sodium hydrogen transporter inhibitor, and a chelator of the extracellular calcium, whereas enhanced by ouabain. Vitamin D receptor (VDR) agonists significantly increased the recruitment of VDR to the vitamin D response element (VDRE) of PTH1R and Klotho promoter, thus increasing the expression of PTH1R and Klotho.

Conclusions: High sodium can decrease the synthesis of active vitamin D in the proximal tubules, affect the gene regulation of 1,25(OH)$_2$D$_3$/VDR, and significantly reduce the expression of PTH1R and Klotho. It revealed the influence of a high-sodium diet on mineral metabolism and the core role of vitamin D in kidney mineral metabolism.

Keywords: High sodium; proximal tubule epithelial cells; 1,25-dihydroxyvitamin D3; parathyroid receptor 1 (PTH1R); Klotho

Submitted Nov 11, 2021. Accepted for publication Mar 10, 2022.
doi: 10.21037/atm-21-5910
View this article at: https://dx.doi.org/10.21037/atm-21-5910

Introduction

Numerous large epidemiologic studies suggest that elevations in the levels of serum phosphate are associated with increased cardiovascular disease (CVD) and mortality in patients with chronic kidney disease (CKD) (1,2) and individuals with normal renal function (3,4). However, in recent decades, phosphate intake has increased due to the growing application of inorganic phosphate additives in processed foods, which is now far above the recommended daily allowance for inorganic phosphate. Thus, maintaining a steady phosphate homeostasis in the general population has

become an increasingly concerning public health problem (5).

Maintenance of phosphate homeostasis depends on the regulation of phosphate handling by bone, intestine, and kidney (5,6), which is coordinately regulated by the parathyroid hormone (PTH), fibroblast growth factor 23 (FGF23), and active vitamin D [1,25$(OH)_2D_3$] (7). The renal threshold for phosphate reabsorption in the proximal tubule is the most important factor in eliminating phosphate loading and maintaining phosphate homeostasis. Phosphate reabsorption in the proximal tubule is mediated by three separate transport proteins, including the sodium phosphate co-transporters type IIa (Npt2a), type IIc (Npt2c), and type III (called Pit-2), of which Npt2, responsible for 70% of phosphate reabsorption in the kidney, is the most important (8,9). In addition to sodium phosphate co-transporters, there are also sodium (Na) hydrogen transporters in the brush border of the proximal tubule, of which sodium hydrogen transporter 3 (NHE3) is responsible for 60% of sodium reabsorption. Through Npt2a or NHE3, sodium enters the proximal tubular epithelial cell during sodium and phosphate reabsorption.

Increasingly, data show that sodium homeostasis may be associated with phosphate homeostasis in animals and humans. For instance, Npt2b and NHE3 are also present in the intestinal epithelial cells. It was found that tenapanor, an inhibitor of the intestinal NHE3, inhibited intestinal sodium absorption and inhibited phosphate reabsorption, resulting in decreased serum phosphate in both maintenance hemodialysis patients and CKD animals (10,11). Moreover, a high-sodium diet could lead to increased intestinal phosphate absorption, increased urinary phosphate excretion, and significantly elevated blood PTH activity in normal rats (12). Similarly, in rat proximal tubule epithelial cells, an acute rise blood pressure (13) or high-sodium diet (14) induced similar changes in the distribution of NHE3 and Npt2a, resulting in a decreased sodium reabsorption. The same distribution change was observed in rats injected with PTH, resulting in decreased Npt2a and NHE3 on the apical side and increased urinary sodium excretion (15). Thus, we speculate that sodium may share the sensing mechanism with phosphate in the proximal tubule and be co-transported by NHE3 and Npt2a.

The proximal tubule is the sensing site of sodium and phosphate and the main place for the synthesis and metabolism of active vitamin D3, a process mainly regulated by 1α-hydroxylase (1α-OHase) and 24-hydroxylase (24-OHase), encoded by the Cyp27b1 and Cyp24a1 genes, respectively. In addition, proximal tubule epithelial cells are also the target cells of active vitamin D_3. Thus, active vitamin D_3 has many potential target genes. In addition, it is a phosphate-regulating factor that can act on PTH and FGF23, and Klotho, thus playing a central role in tubular phosphate regulation.

Studies have shown that high-phosphate loading can reduce the synthesis of active vitamin D_3 in proximal tubules (16,17). However, sodium may share the sensing mechanism with phosphate in the proximal tubule epithelial cells, and whether sodium cooperates with phosphate or operates independently in the regulation of phosphate homeostasis remains unknown. Therefore, in this *in vitro* study, we investigated the effects of high sodium on the synthesis and function of active vitamin D and the local phosphate regulation in proximal tubular epithelial cells. We present the following article in accordance with the MDAR reporting checklist (available at https://atm.amegroups.com/article/view/10.21037/atm-21-5910/rc).

Methods

Cell culture and treatment

Human proximal tubule epithelial (HK-2: ATCC Cat# CRL-2190, RRID:CVCL_0302) cells were purchased from Nanjing KeyGen Biotech Co., Ltd., Nanjing, China. The cells were maintained in DMEM/ F12 medium (Gibco; Thermo Fisher Scientific, MA, USA) plus 10% fetal calf serum (FBS) and 1% penicillin/streptomycin. After culture of the confluent or subconfluent cells, the cells were made quiescent in DMEM/F12 medium with 0.5% FBS for 24 hours. Quiescent cells were treated with different concentrations of phosphate/sodium with or without the sodium-dependent phosphate transporter inhibitor phosphonoformic acid trisodium salt hexahydrate (PFA, 1 mM/L) and/or sodium/hydrogen exchanger inhibitor cariporide (0.2 mM/L), ouabain (10 nM/L), or ethylene glycol tetraacetic acid (EGTA) or different concentrations of vitamin D receptor agonist (VDRA) calcitriol (Sigma) for 24 hours.

Vitamin D receptor (VDR) gene silencing by RNA interference

A lentiviral expression vector (GV248, Genechem, Shanghai, China) and a lentiviral control expression vector were used to ensure transfection efficiency. Lentivirus-expressing shRNAs were generated using hU6-MCS-

Ubiquitin-EGFP-IRES-puromycin. Transfections were performed according to the manufacturer's instructions. Briefly, the HK-2 cells used in this experiment were grown in 12-well plates and transfected at 50–70% confluence. Before sh*VDR* transfection, the medium was changed to serum-free medium, and HitransG A or P transfection reagent (Genechem, Shanghai, China) was used in VDR interference to ensure transfection efficiency. Cells were further incubated for an additional 72 h before the experimental assays. The silencing efficiency of sh*VDR* transfections was confirmed by observing the fluorescence expressed by EGFP. In addition, the protein level was verified by Western blotting, and real-time polymerase chain reaction (RT-PCR) was carried out.

Quantitative RT-PCR

Total RNA was extracted from HK-2 cells following the protocols of Trizol reagent (Invitrogen, CA, USA). The concentration and purity of the extracted total RNA was determined utilizing a microplate reader. The reagents and samples involved were placed on ice, and miRNA reverse transcription was performed on ice. The reaction system of reverse transcription is shown in Table S1. According to the manufacturer's instructions, after centrifugation (42 ℃, 60 min) and degeneration under 95 ℃ for 3 min, miRNA reverse transcription was terminated at 4 ℃. Prepared cDNA was immediately subjected to PCR. A SYBR Green Premix Kit (BIOTNT, China) was used for RT-PCR. mRNA reverse transcription system is listed in Tables S2. The relative gene expression levels were calculated using the $2^{-\Delta\Delta CT}$ method (17), and GAPDH or βactin was used as the reference gene. The expressions of the two reference genes were constant and stable. The sequences, accession number and hybridization positions of primers used for amplification were shown in *Table 1*.

Western blot

The cells were washed with phosphate-buffered saline (Invitrogen, CA) and harvested by the RIPA containing 10% phenylmethanesulfonyl fluoride (PMSF). Cell extracts were centrifuged at 12,000 rpm at 4 ℃ for 20 min in a high-performance centrifuge (20R, Beckman Counter, CT, USA). The protein concentration of each sample was determined by multivolume Spectrophotometer (Epoch, USA). Twenty μg proteins were separated on SDS-PAGE. After complete electrophoresis, the proteins were transferred into PVDF membranes (Millipore, Billerica, MA, USA). After blocking with 5% nonfat milk or BSA, membranes were incubated with the following antibodies overnight at 4 ℃: anti-1α-OHase (1:1,000; Abcam Cat# ab206655, RRID:AB_2894966), anti-24-OHase (1:500; Affinity Biosciences Cat# DF3568, RRID:AB_2835940), anti-parathyroid receptor 1 (anti-PTH1R) (1:200, Santa Cruz Biotechnology Cat# sc-12722, RRID:AB_628188), anti-Klotho (1:500; Affinity Biosciences Cat# DF10309, RRID:AB_2840887), and anti-GAPDH (1:1,000, Santa Cruz Biotechnology Cat# sc-47724, RRID:AB_627678). Then the membranes were incubated with horseradish peroxidase-conjugated secondary antibodies for 1 hour at room temperature. ECL Western blotting detection reagent was used for exposure and development with a GE Image Quant LAS 4000 (CA, USA). Bands were quantified by densitometry using Image J 1.40 g software.

Immunofluorescence analysis

For imaging experiments, HK-2 cells were cultured on coverslips. At the end of the treatments, cells were fixed in 4% paraformaldehyde and processed for immunostaining. To evaluate PTH1R and VDR expression, cells were incubated overnight at 4 ℃ with mouse anti-PTH1R (1:200, Santa Cruz Biotechnology Cat# sc-12722, RRID:AB_628188) and mouse anti-VDR (1:100; Abcam Cat# ab89626, RRID:AB_2212490) and washed three times with 1× PBS followed by incubation with a secondary goat anti-mouse IgG antibody (1:200; Millipore) or a secondary goat anti-mouse antibody conjugated with Cyc2 (1:100; Jackson) for 2 hours at room temperature. Subsequently, 4',6-diamidino-2-phenylindole (DAPI; Sigma-Aldrich, D8417) was used to stain the nuclei. Images were acquired on a fluorescence microscope (Nikon, Japan).

Detection of 1,25(OH)$_2$D$_3$ using liquid chromatography/mass spectrometry (LC/MS)

To measure the ability of these cells to convert 25-(OH) D_3 into 1,25-$(OH)_2D_3$, 20 mM 25-hydroxyvitamin D_3 monohydrate was added to the medium and the cells were incubated for 6 h. The reaction was stopped by freezing at –20 ℃, and the culture mixture was scraped and collected. Then 1 ml of N-hexane/ethyl acetoacetate mixture (9:1) was added, followed by vigorous mixing for 1 min. After centrifuging at 23,708 ×g at 4 ℃ for 10 min in a high-performance centrifuge (Avanti J-26S, Beckman Counter),

Table 1 The sequences and accession number of primers used for amplification

Gene	Product length	Primer sequences and hybridization positions of primers				Accession number
		Primer	5'	Sequences	3'	
GAPDH	105	F	1	GGGAAGGTGAAGGTCGGAGT	20	NM_001357943.2
		T	80		99	
		R	1	GGGGTCATTGATGGCAAC	18	
		T	184		167	
βactin	103	F	1	CTTCGCGGGCGACGAT	16	NM_001101.5
		T	144		159	
		R	1	CACATAGGAATCCTTCTGACCC	22	
		T	246		225	
Cyp27b1	92	F	1	AGTTGCTATTGGCGGGAGTG	20	NM_000785.4
		T	975		994	
		R	1	GAGTGCTGTCTGGACTTCGG	20	
		T	1,066		1,047	
Cyp24a1	164	F	1	AGGCCACGTTGAAGACTTGT	20	NM_001128915
		T	998		1,017	
		R	1	TCCTCCCAAACGTGCTCATC	20	
		T	1,161		1,142	
VDR	114	F	1	GACCTCACAGAAGAGCACCC	20	NM_001017535.2
		T	190		209	
		R	1	CGTTCCGGTCAAAGTCTCCA	20	
		T	303		284	
RXRα	184	F	1	CAGGGGCTCCCTTTTCTGTG	20	NM_001291920.2
		T	721		740	
		R	1	GGAGGTGAGGGAGGAGTTCA	20	
		T	904		885	
Klotho	198	F	1	TGGATCACCATCGACAACCC	20	NM_004795.4
		T	718		737	
		R	1	GCTTAGGGCAATGGACACCT	20	
		T	915		896	
FGFR1	121	F	1	GCCCAGACAACCTGCCTTAT	20	NM_001354367.2
		T	1,037		1,056	
		R	1	CACGTATACTCCCCTGCGTC	20	
		T	1,157		1,138	
PTH1R	118	F	1	AGGGACTATCCATGGCCTCC	20	NM_000316.3
		T	41		60	
		R	1	CCACTCTTCGGCTGTCTGG	19	
		T	158		140	

F, forward primer; T, template; R, reverse primer.

the supernatant was transferred to an Eppendorf tube and dried on a nitrogen platform at room temperature. The precipitate was resuspended in a 100-mL methanol/water (1:1) mixture and analyzed using LC/MS.

Detection of 1,25(OH)$_2$D$_3$ by enzyme-linked immunosorbent assay (ELISA)

25-hydroxyvitamin D_3 monohydrates were added to the cell medium (at a final concentration of 20 mM) and incubated for 24 or 48 h. The reaction was stopped by freezing at –20 ℃, the culture mixture was scraped and collected in a centrifuge tube, and then 1,25$(OH)_2D_3$ were esterified and extracted from the cell culture mixture using the ELISA kit (IDS, UK). The collected fractions were dried under a steady stream of nitrogen gas. Residues were reconstituted in 100 mL buffer, then incubated with the 1,25$(OH)_2D_3$ antibody overnight at 4 ℃. Finally, the reaction was stopped by a stop solution and analyzed using a chemiluminescence immune detection system with excitation at 494 nm.

Electrophoretic mobility shift assay (EMSA)

Cells were harvested and homogenized in the manner mentioned above. After 15 minutes on ice, PMSF was added to the homogenate to a final concentration of 10%, and the mixture was vortexed and microfuged (10,000 rpm) for 1 minute at 4 ℃. The nuclear pellet was resuspended in ice-cold hypertonic nuclear extraction buffer, incubated on ice for 30 minutes with intermittent vortexing, and microfuged (10,000 rpm) for 5 minutes at 4 ℃. The supernatant containing the nuclear extract was collected, and a 2-mL nuclear extract was incubated for 20 minutes at 37 ℃ with 1 mL labeled probe and 1 mL Cyp24a1 antibody. Bound complexes were separated on 6.5% acrylamide gel with Tris-glycine running buffer, and then assessed using a G: BOX ChemiXR5 Gel imaging system.

RNA sequencing and bioinformatics analysis

Three independent plates of HK-2 cells were treated or not treated with phosphate (4 mM) or NaCl (170 mM) for 24 h. Total RNA was reversely transcribed into double-stranded cDNA, then synthesized to cRNA labeling with Cy3. The gene chip tests were performed by the Shanghai Oebitech Company (Shanghai, China). Quintile normalization and subsequent data processing were done through Gene Spring GX software. The RUV-normalized expression data is available through the Gene Expression Omnibus (GEO; https://www.ncbi.nlm.nih.gov/geo/) and can be accessed via the GSE series number GSE124814. cRNAs with a 1.5-fold change in expression were considered differentially expressed and are shown in the heatmap ($P<0.05$). The cRNAs that showed consistent results in these two screenings were selected as potential target cRNAs. Molecular function and classification of differentially expressed genes (DEGs) were analyzed with Gene Ontology (GO) and Kyoto Encyclopedia of Genes and Genomes (KEGG) pathways using the Database for Annotation, Visualization, and Integrated Discovery Bioinformatics Resources (https://david.ncifcrf.gov).

Intracellular Ca^{2+} detection

Intracellular Ca^{2+} was detected with the Ca^{2+} indicator dye Fura-4. Briefly, cells plated on a 12-well-plate were incubated at 37 ℃ for 60 min in Hank's balanced salt solution (HBSS) containing 5 mol/L Fura-4 acetoxymethyl ester (AM). The medium was then thoroughly removed, and the cells were washed with HBSS solution three times to reduce the influence of phenol red in the medium on the probe. After perfusion of HBSS for 25 min to completely de-esterify the AM, the fluorescence of cells with excitation at 494 nm and emission at 516 nm was measured using a fluorescence microscope.

Chromatin immunoprecipitation (ChIP)

ChIP assays were performed using an EpiQuik TM Chromatin Immunoprecipitation kit. Briefly, different groups of cells were crosslinked with 1% formaldehyde. Crosslinking was terminated using 1.25 M glycine. The cells were added to the homogenizing buffer, triturated, disaggregated, and centrifuged at 1,000 g for 5 min at 4 ℃. After the removal of supernatants, protease inhibitors were added, and the disaggregated parts were resuspended. Chromatin was sheared by sonication. Immunoprecipitation was performed at room temperature for 90 min. The specific VDR antibodies for ChIP were purchased from Santa Cruz. Crosslinking was reversed at 65 ℃ for 90 min. Finally, genomic DNA was eluted for PCR analysis. Thermocycler conditions were 94 ℃ for 4 min, then

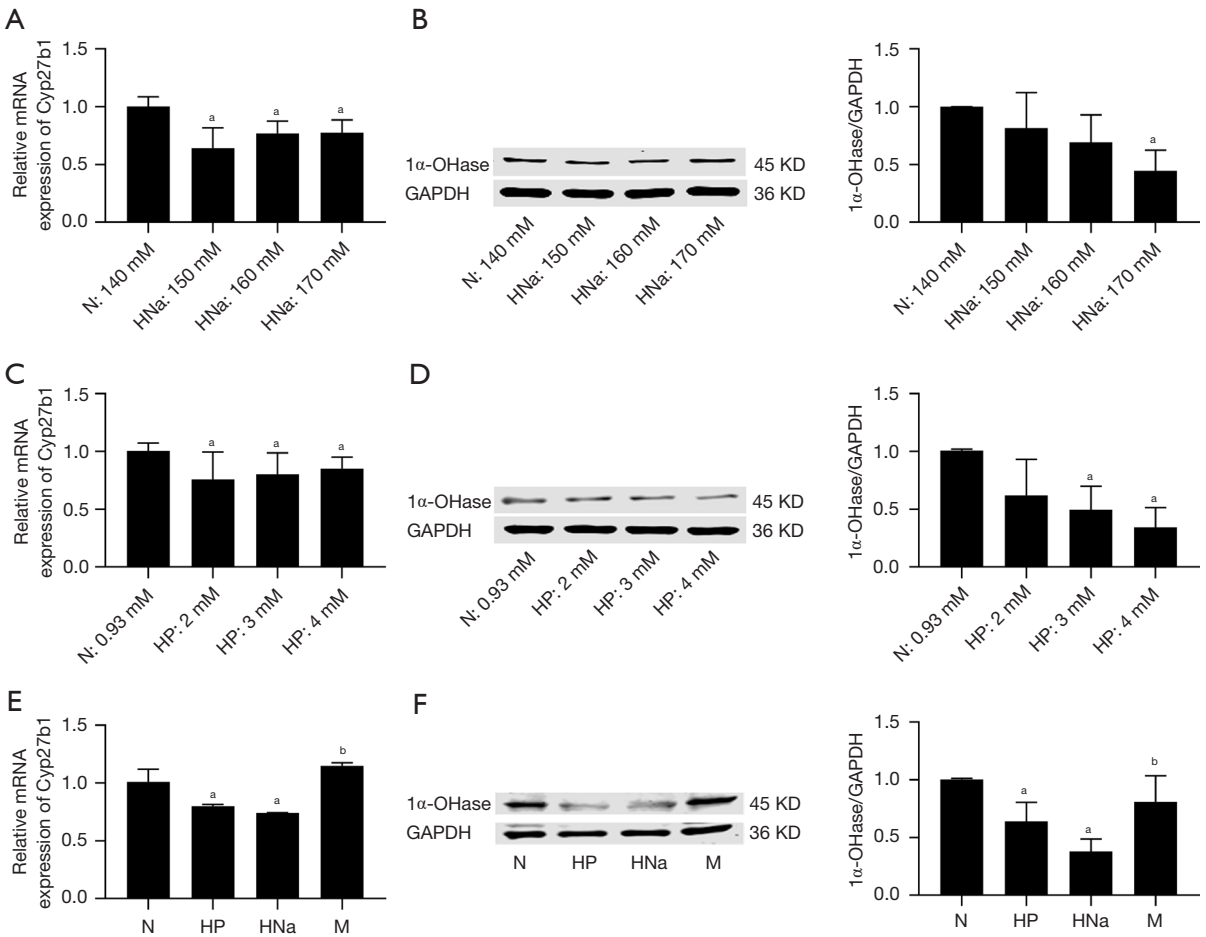

Figure 1 High sodium reduced the expression of 1α-OHase (Cyp27b1) in HK-2 cells. (A,B) mRNA and protein expression of Cyp27b1 in HK-2 cells after incubation in different concentrations of sodium (140/150/160/170 mM) for 24 hours. (C,D) mRNA and protein expression of Cyp27b1 in HK-2 cells after incubation in different concentrations of phosphate (0.93/2/3/4 mM) for 24 hours. (E,F) mRNA and protein expression of Cyp27b1 in HK-2 cells after incubation in N, HP (4 mM), HNa (170 mM), and M with the same osmotic pressure for 24 hours. [a], versus N, P<0.05; [b], versus HNa, P<0.05. HK-2, human proximal tubule epithelial cell; N, normal medium; HP, high phosphate; HNa, high sodium; M, mannitol.

40 cycles of 30 s at 94 ℃, 30 s at 60 ℃ and 90 s at 72 ℃.

Statistical analyses

All values are expressed as mean ± SD for at least three separate experiments. Statistical analysis was performed by Student *t*-test, one-way analysis of variance (ANOVA), and the Tukey-Kramer post hoc test as appropriate using Prism 7.0 (GraphPad, San Diego, CA, USA). Values with a P<0.05 were considered statistically significant.

Results

Effects of high sodium on the expression of 1α-OHase, 24-OHase and 1,25(OH)$_2$D$_3$ in HK-2 cells

High sodium reduces the expression of 1α-OHase (Cyp27b1) in HK-2 cells

After incubation in different concentrations of sodium (140/150/160/170 mM) for 24 hours, the mRNA and protein expression of 1α-OHase (Cyp27b1) in HK-2 cells decreased (*Figure 1A,1B*), which was similar to the

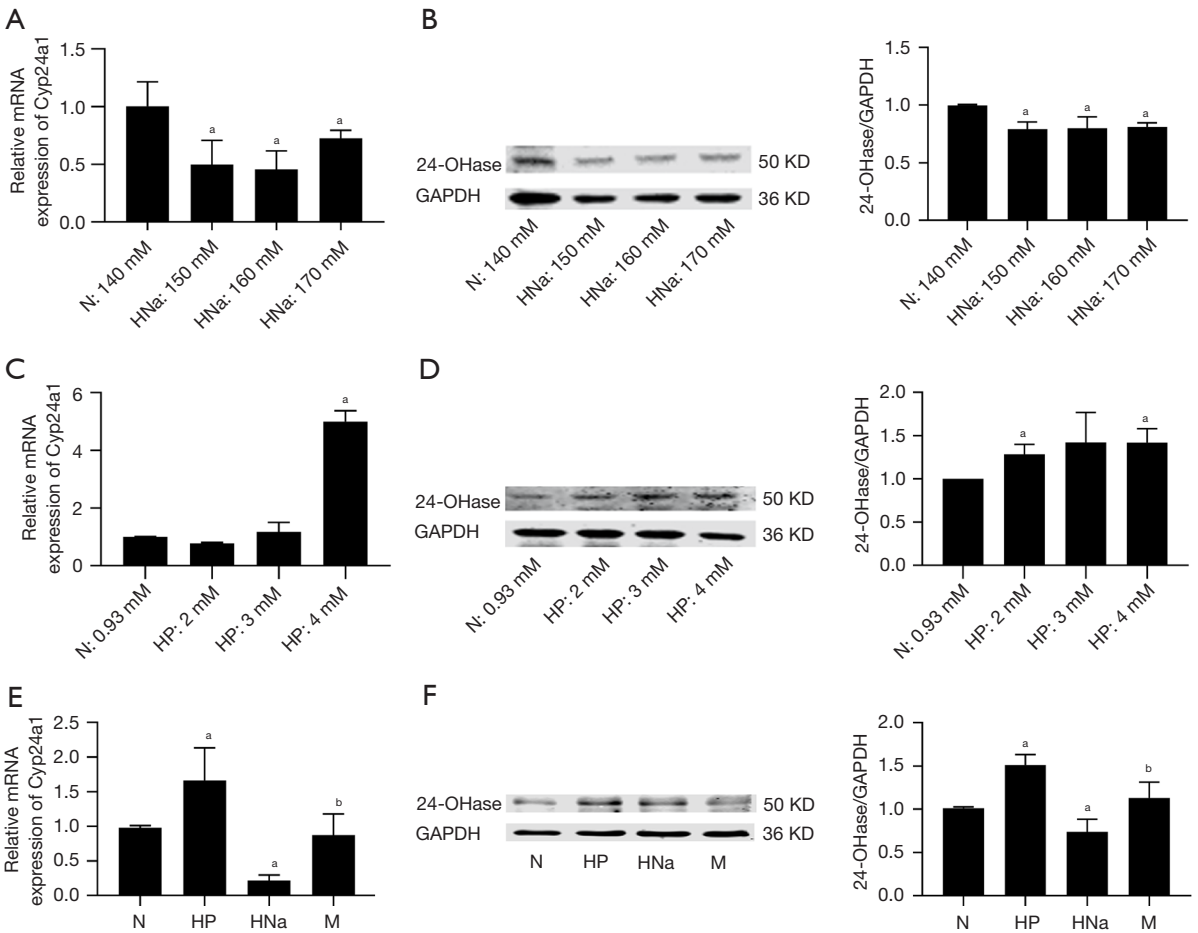

Figure 2 High sodium reduced the expression of 24-OHase (Cyp24a1) in HK-2 cells. (A,B) mRNA and protein expression of Cyp24a1 in HK-2 cells after incubation in different concentrations of sodium (140/150/160/170 mM) for 24 hours. (C,D) mRNA and protein expression of Cyp24a1 in HK-2 cells after incubation in different concentrations of phosphate (0.93/2/3/4 mM) for 24 hours. (E,F) mRNA and protein expression of Cyp24a1 in HK-2 cells after incubation in N, HP (4 mM), HNa (170 mM) and M with the same osmotic pressure for 24 hours. [a], versus N, P<0.05; [b], versus HNa, P<0.05. HK-2, human proximal tubule epithelial cell; N, normal medium; HP, high phosphate; HNa, high sodium; M, mannitol.

results of high-phosphate (0.93/2/3/4 mM) intervention (*Figure 1C,1D*). Furthermore, it was found that the effect of high sodium (170 mM) on reducing 1α-OHase is not related to osmotic pressure because mannitol with the same osmotic pressure has no such effect (*Figure 1E,1F*).

High sodium reduces the expression of 24-OHase (Cyp24a1) in HK-2 cells

High sodium decreased the mRNA and protein expression of 24-OHase (Cyp24a1) in HK-2 cells (*Figure 2A,2B*), whereas high-phosphate intervention increased the mRNA and protein expression of 24-OHase (Cyp24a1) (*Figure 2C,2D*). Similarly, the effect of high sodium (170 mM) was not due to osmotic pressure (*Figure 2E,2F*).

High sodium decreases the expression of $1,25(OH)_2D_3$ in HK-2 cells

After incubation with $25(OH)D_3$ substrate, the HK-2 cells could synthesize $1,25(OH)_2D_3$, which was confirmed by the results of LC/MS (*Figure 3A*). Furthermore, the ELISA results revealed that high-sodium intervention reduced the expression of $1,25(OH)_2D_3$, which was similar to the effects

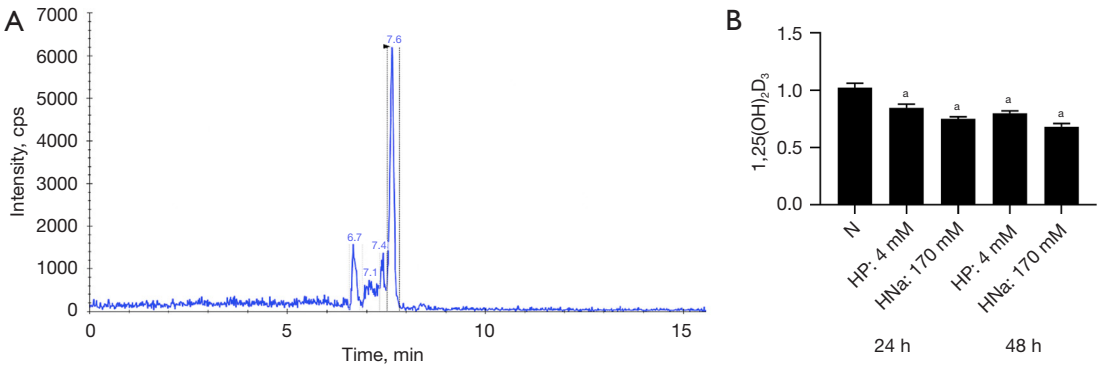

Figure 3 High sodium decreased the expression of $1,25(OH)_2D_3$ in HK-2 cells. (A) LC/MS result showed that HK-2 cells could synthesize $1,25(OH)_2D_3$. (B) ELISA result of $1,25(OH)_2D_3$ expressions in HK-2 cells after incubation in N, HP (4 mM), HNa (170 mM) for 24 and 48 hours. [a], versus N, P<0.05. HK-2, human proximal tubule epithelial cell; LC/MS, liquid chromatography mass spectrometry; ELISA, the enzyme-linked immunosorbent assay; N, normal medium; HP, high phosphate; HNa, high sodium.

of high-phosphate (*Figure 3B*).

Effects of altering membranous sodium transporters on the expression of 1α-OHase (Cyp27b1) and 24-OHase (Cyp24a1) in HK-2 cells

Sodium and phosphate related transporter inhibitors increase the expression of 1α-OHase (Cyp27b1) and 24-OHase (Cyp24a1) in HK-2 cells

Since Npt2a and NHE3 are the two most important transporters mediating the entry of extracellular sodium in the cell, to explore the mechanisms of extracellular sodium, the sodium phosphate transporter inhibitor (PFA) and sodium hydrogen transporter inhibitor (cariporide) were used together to reduce intracellular sodium concentration comprehensively. In the presence of PFA and cariporide, even under high sodium or high phosphate, the mRNA and protein expression of 1α-OHase (Cyp27b1) were significantly higher than in the normal controls (*Figure 4A,4B*). Furthermore, the combined effects of PFA and cariporide also significantly increased the expression of 24-OHase (Cyp24a1) compared with the control, the high sodium group, and the high-phosphate group (*Figure 4C,4D*).

Ouabain decreases the expression of 1α-OHase (Cyp27b1) and 24-OHase (Cyp24a1) in HK-2 cells

Ouabain can increase the intracellular sodium concentration. However, regardless of the application of ouabain alone or ouabain combined with high sodium/high phosphate, the mRNA and protein expression of 1α-OHase (Cyp27b1; *Figure 5A,5B*) and 24-OHase (Cyp24a1; *Figure 5C,5D*) in HK-2 cells were significantly lower than those in the high-sodium/high-phosphate group, suggesting that sodium played an important role in reducing the expression of 1α-OHase and 24-OHase.

High sodium affected the expression of 1α-OHase (Cyp27b1) and 24-OHase (Cyp24a1) by promoting extracellular calcium influx

Bioinformatics analysis of DEGs in HK-2 cells after high-sodium/high-phosphate intervention

After high sodium or high-phosphate intervention, 1,449 DEGs jointly affected by high sodium and high phosphate were identified (*Figure 6A*). KEGG enrichment analysis was performed on 703 annotated genes, indicating that the high sodium and phosphate intervention affected calcium signaling pathways, glutamatergic synapses, cardiac muscle contraction, and complement and coagulation cascades (*Figure 6B*). The significant GO biological processes of DEGs were calcium ion import, calcium ion transport into the cytosol, and calcium ion transmembrane transport (*Figure 6C*). Taken together, these data suggested that high sodium/high phosphate might work by increasing intracellular calcium ions in proximal tubule epithelial cells.

High sodium increases intracellular calcium concentration in HK-2 cells

Intracellular calcium content increased after high sodium/high-phosphate intervention. Using sodium phosphate transporter inhibitor and sodium hydrogen transporter

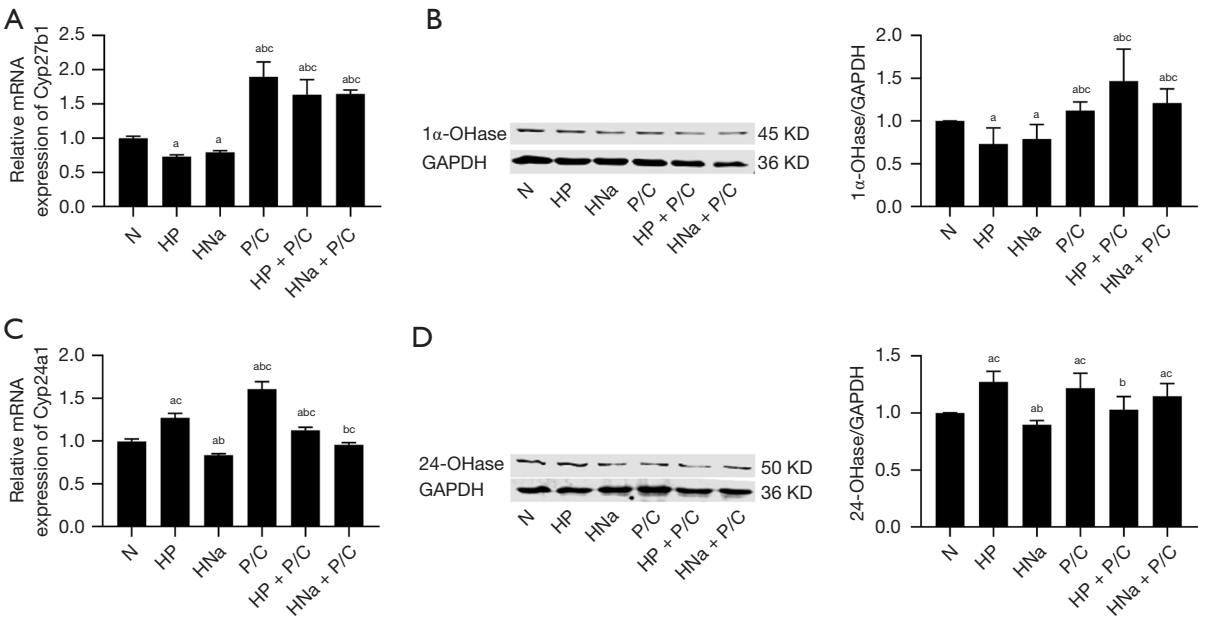

Figure 4 Effects of sodium phosphate transporter inhibitor (PFA) and sodium hydrogen transporter inhibitor (cariporide) on the expression of 1α-OHase (Cyp27b1) and 24-OHase (Cyp24a1) in HK-2 cells. (A,B) mRNA and protein expression of Cyp27b1 in HK-2 cells after incubation in N, HP (4 mM), HNa (170 mM), P/C, HP + P/C and HNa + P/C for 24 hours. (C,D) mRNA and protein expression of Cyp24a1 in HK-2 cells after incubation in N, HP (4 mM), HNa (170 mM), P/C, HP + P/C and HNa + P/C for 24 hours. [a], versus N, P<0.05; [b], versus HP, P<0.05; [c], versus HNa, P<0.05. PFA, phosphonoformic acid trisodium salt hexahydrate; HK-2, human proximal tubule epithelial cell; N, normal medium; HP, high phosphate; HNa, high sodium; P/C, phosphonoformic acid trisodium salt hexahydrate + cariporide; HP + P/C, high phosphate + phosphonoformic acid trisodium salt hexahydrate + cariporide; HNa + P/C, high sodium + phosphonoformic acid trisodium salt hexahydrate + cariporide.

inhibitor combined with high phosphate/high sodium significantly decreased the intracellular calcium content. In contrast, ouabain combined with high phosphate/high sodium increased the intracellular calcium content (*Figure 7*).

Chelating extracellular sodium reverses high sodium-induced 1α-OHase (Cyp27b1) and 24-OHase (Cyp24a1) downregulation

Compared with the high sodium group, high sodium combined with EGTA increased the gene and protein expression of 1α-OHase (Cyp27b1) and 24-OHase (Cyp24a1). Similarly, compared with the high-phosphate group, high phosphate combined with EGTA increased the expression of 1α-OHase (Cyp27b1) and decreased the expression of 24-OHase (Cyp24a1) (*Figure 8*). Thus, the results indicated that high sodium/high phosphate affects the expression of 1α-OHase (Cyp27b1) and 24-OHase (Cyp24a1) by promoting extracellular calcium influx.

Effects of high sodium on vitamin D regulatory target genes

High sodium reduces, while VDRA promotes, the binding ability of VDR/RXRα to the vitamin D response element (VDRE) of *Cyp24a1*

High sodium had no effects on the gene and protein expression of VDR and RXRα (data not shown). EMSA results showed that compared with the control group, high sodium could reduce the binding ability of VDR/RXRα to the VDRE of target gene *Cyp24a1*. VDRA could significantly promote the binding ability of VDR/ RXRα to the VDRE of target gene *Cyp24a1*. At the same time, this effect could be reduced by combining VDRA and high sodium/high phosphate (*Figure 9*).

High sodium-reduced, while VDRA increased, the expression of PTH1R

Compared with the control group, the gene and protein expression of PTH1R decreased after high sodium

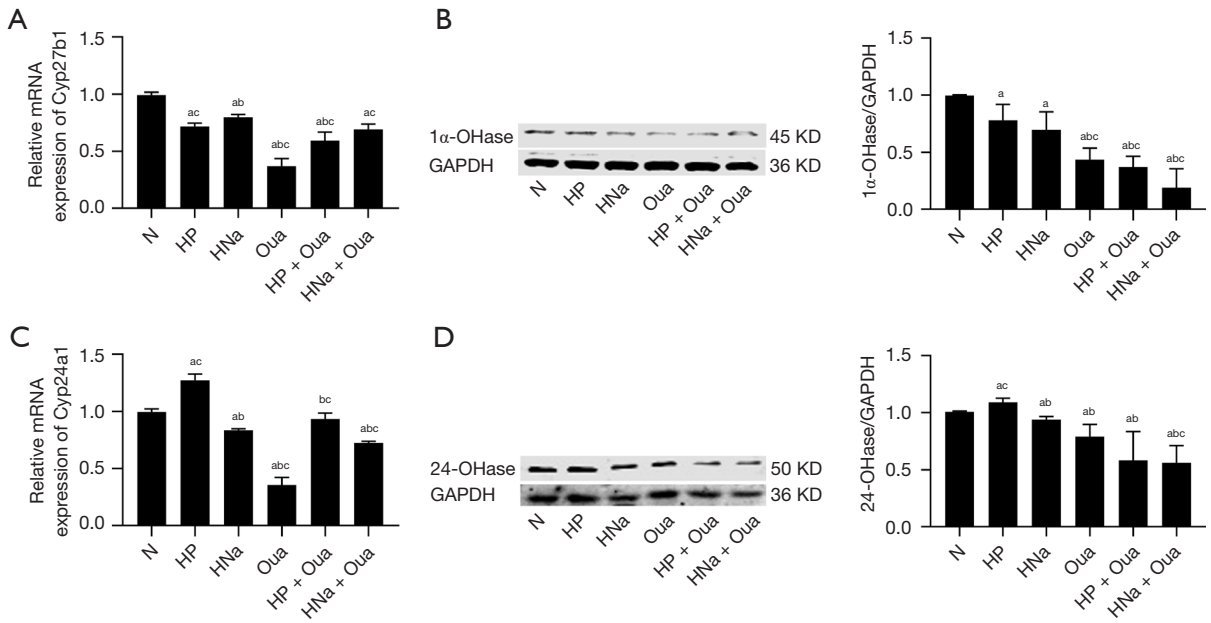

Figure 5 Ouabain decreased the expression of 1α-OHase (Cyp27b1) and 24-OHase (Cyp24a1) in HK-2 cells. (A,B) mRNA and protein expression of Cyp27b1 in HK-2 cells after incubation in N, HP (4 mM), HNa (170 mM), Oua, HP + Oua and HNa + Oua for 24 hours. (C,D) mRNA and protein expression of Cyp24a1 in HK-2 cells after incubation in N, HP (4 mM), HNa (170 mM), Oua, HP + Oua and HNa + Oua for 24 hours. [a], versus N, P<0.05; [b], versus HP, P<0.05; [c], versus HNa, P<0.05. HK-2, human proximal tubule epithelial cell; N, normal medium; HP, high phosphate; HNa, high sodium; Oua, ouabain; HP + Oua, high phosphate + ouabain; HNa + Oua, high sodium + ouabain.

intervention. Immunofluorescence results showed that PTH1R was mainly expressed in the membrane and cytoplasm (*Figure 10*). After the administration of PFA and Cariporide, the mRNA and protein expression of PTH1R were significantly increased (*Figure 10A,10B*). In contrast, the PTH1R expression decreased further with the high-Na/high-phosphate group (*Figure 10C,10D*). Active vitamin D_3 could significantly increase the gene and protein expression of PTH1R, while *VDR* shRNA reduced the expression of PTH1R (*Figure 10E-10G*).

In addition, the results of chromatin immunoprecipitation showed that VDRA significantly increased the recruitment of VDR/RXRα to the VDRE of PTH1R promoter compared with the control group, while the combination of high sodium/high phosphate and VDRA could reduce the relative recruitment (*Figure 11*).

High sodium decreased the expression of Klotho

High sodium/high phosphate does not affect gene and protein expression of fibroblast growth factor receptor (FGFR) (data not shown). High sodium decreased Klotho's gene and protein expression compared with the control group (*Figure 12*). The combined use of PFA and Cariporide could significantly increase Klotho's gene and protein expression (*Figure 12A,12B*). At the same time, ouabain intervention could further decrease Klotho's gene and protein expression (*Figure 12C,12D*). VDRA could significantly increase Klotho's gene and protein expression compared with the control and high sodium/high-phosphate groups (*Figure 12E,12F*).

Discussion

The present study demonstrated that high sodium/high phosphate is co-transported through Npt2a and NHE3 in HK-2 cells, which increases the intracellular calcium content and directly inhibits $1,25(OH)_2D_3$ synthesis. In addition, high sodium/high phosphate can affect the gene regulation of $1,25(OH)_2D_3$/VDR by inhibiting the synthesis of $1,25(OH)_2D_3$, and significantly reduce the expression of PTH1R and Klotho, an effect that can be reversed by the application of VDRA.

Proximal tubule epithelial cells are the main sites of $1,25(OH)_2D_3$ synthesis and metabolism. We could detect

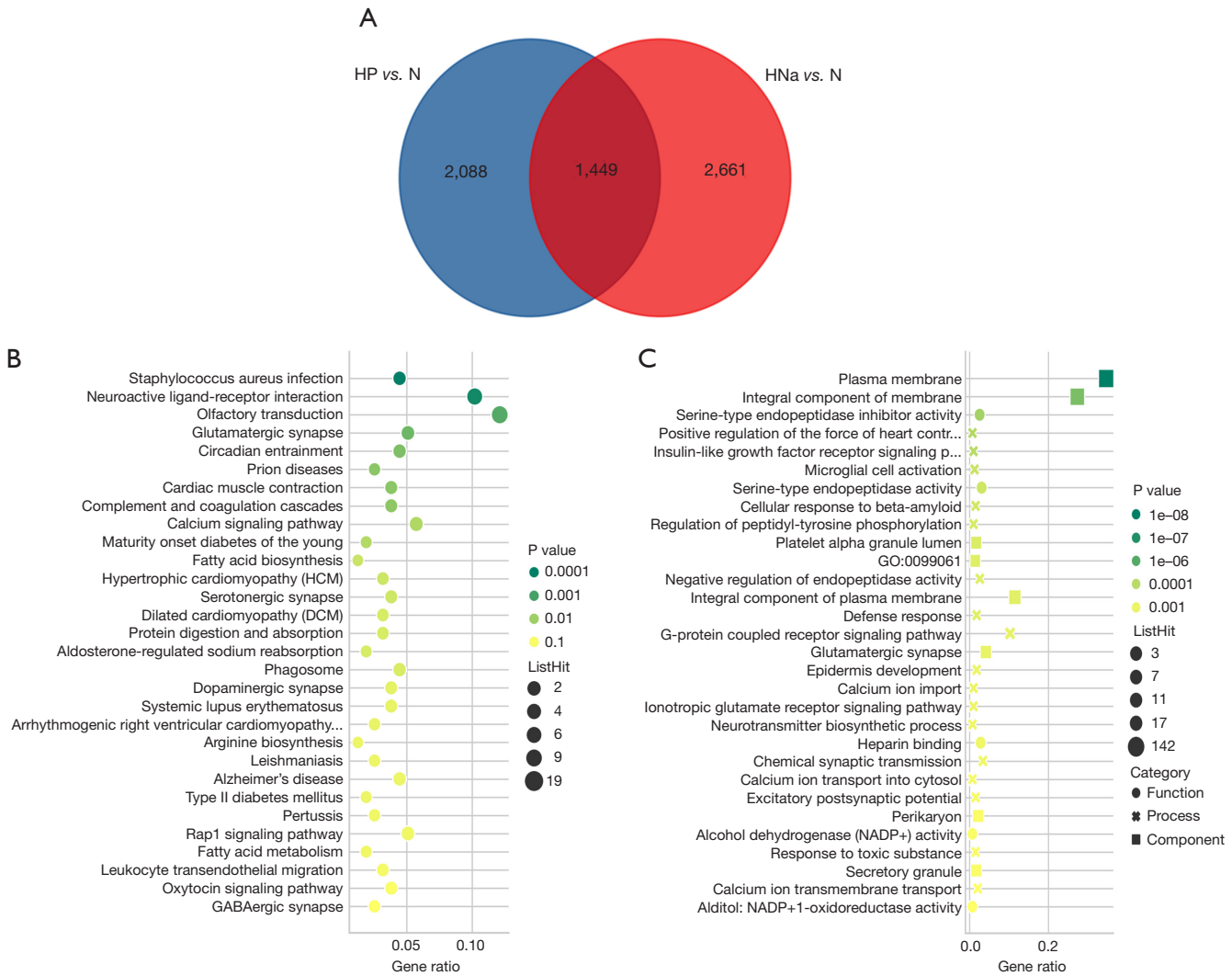

Figure 6 Bioinformatics analysis of DEGs in HK-2 cells after high sodium/HP intervention. (A) Venn diagram of DEGs jointly affected by high sodium and high phosphate. (B) GO enrichment analysis of 1,449 DEGs. (C) KEGG pathways analysis of 1,449 DEGs. N, normal medium; HP, high phosphate; HNa, high sodium; HK-2, human proximal tubule epithelial cell; DEGs, differentially expressed genes; GO, Gene Ontology; KEGG, Kyoto Encyclopedia of Genes and Genomes.

the final synthesis of $1,25(OH)_2D_3$ by adding $25(OH)D_3$ substrate to cultured human proximal tubule epithelial cells, consistent with the previous observation that cultured primary rabbit proximal tubule epithelial cells could synthesize active vitamin D_3 *in vitro* (18). The levels of $1,25(OH)_2D_3$ is closely related to the two enzymes. 1α-OHase is mainly distributed in proximal tubule epithelial cells with the effects of hydroxylating $25(OH)D_3$ to $1,25(OH)_2D_3$, and plays the most important role in the production of $1,25(OH)_2D_3$. At the same time, 24-OHase (Cyp24a1) is widely expressed in various cells and plays a role in the degradation of $1,25(OH)_2D_3$. The Cyp24a1 pathway is the main route for the catabolism of 1,25(OH)2D3, while other pathways also exist including epimerization, alternative Cyp11a1 metabolites, and conjugation (19,20). Many studies have found that a high phosphate diet could decrease the levels of $1,25(OH)_2D_3$ in humans (21-23), but there are few studies on the effect of a high sodium diet on $1,25(OH)_2D_3$. Animal studies have shown that a high sodium diet could significantly reduce the mRNA expression of Cyp27b1 in the kidney and decrease the expression of Cyp24a1 while not reaching statistical

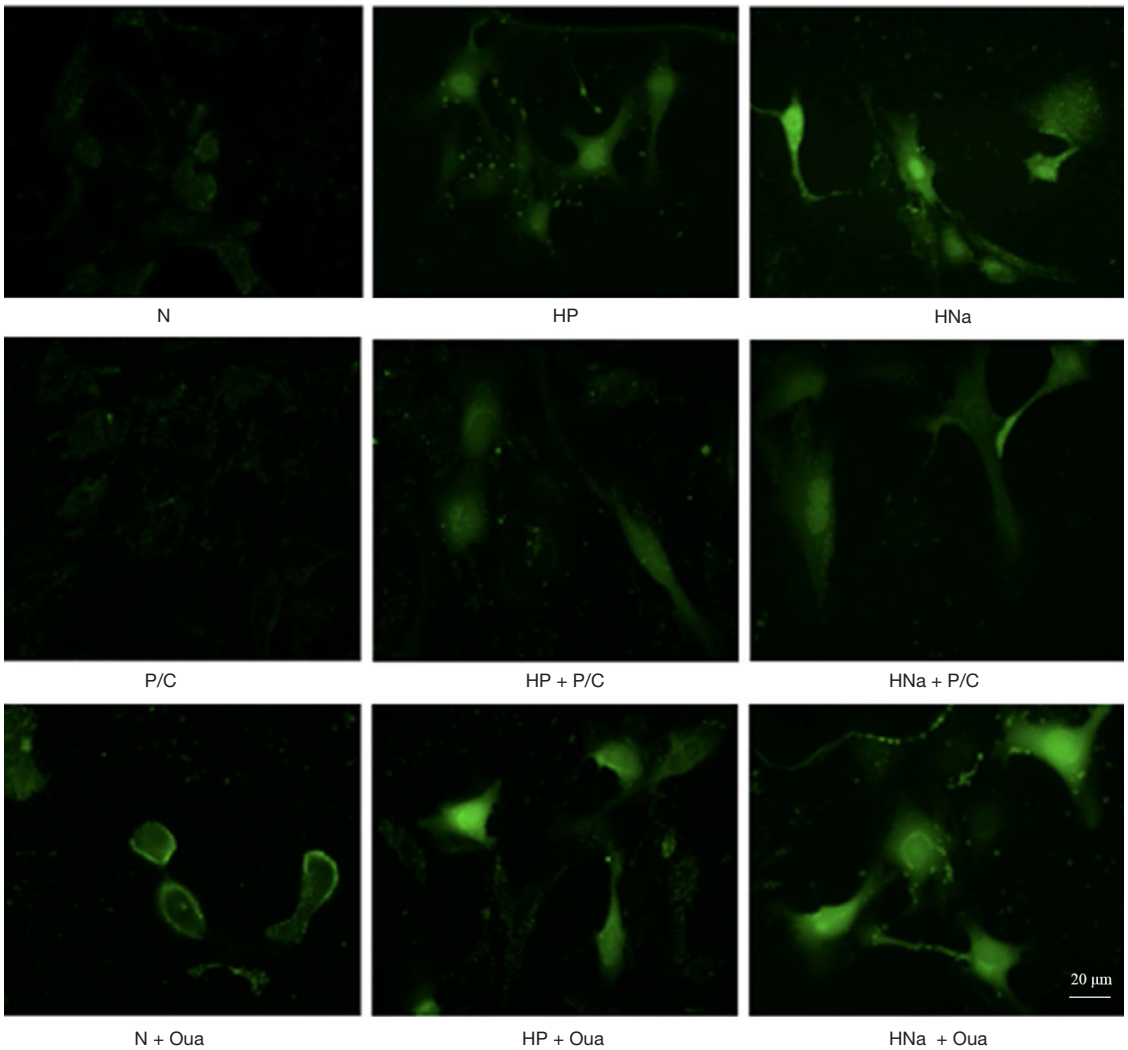

Figure 7 Effects of high sodium and HP intervention on intracellular calcium concentration in HK-2 cells. The fluorescence of Ca^{2+} indicator dye Fura-4 in HK-2 cells cultured in N, HP (4 mM), HNa (170 mM), P/C, HP + P/C, HNa + P/C, N + Oua, HP + Oua and HNa + Oua. HK-2, human proximal tubule epithelial cell; N, normal medium; HP, high phosphate; HNa, high sodium; PFA, phosphonoformic acid trisodium salt hexahydrate; P/C, phosphonoformic acid trisodium salt hexahydrate + cariporide; HP + P/C, high phosphate + phosphonoformic acid trisodium salt hexahydrate + cariporide; HNa + P/C, high sodium + phosphonoformic acid trisodium salt hexahydrate + cariporide; N + Oua, normal medium + ouabain; HP + Oua, high phosphate + ouabain; HNa + Oua, high sodium + ouabain.

significance (24). Our results revealed that high phosphate could reduce the expressions of $1,25(OH)_2D_3$ by reducing 1α-OHase and increasing 24-OHase, and high sodium could also reduce the synthesis of $1,25(OH)_2D_3$ by reducing 1α-OHase. In addition, high sodium down-regulated the expression of 24-OHase, and the overall effects of high sodium was decreasing the expression of $1,25(OH)_2D_3$, suggesting the reduction of 1α-OHase played the predominant role in inhibiting $1,25(OH)_2D_3$ production.

We further verified the role of high sodium in regulating $1,25(OH)_2D_3$ synthesis in proximal epithelial cells by changing the sodium transport on the membrane. Npt2a and NHE3 are the two most important transporters for the entry of extracellular sodium into cells. After the combined application of sodium phosphate transporter inhibitor and sodium hydrogen transporter inhibitor to fully reduce the intracellular sodium, the expression of 1α-OHase was significantly increased. In addition, the expression of

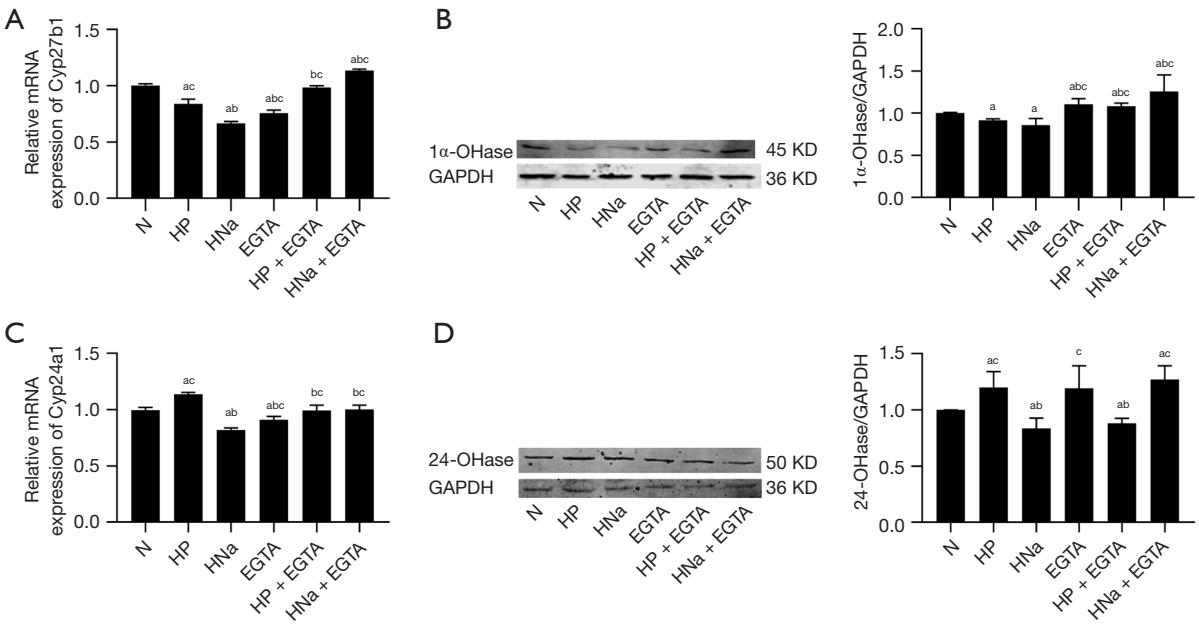

Figure 8 Chelating extracellular calcium reversed high sodium-induced 1α-OHase (Cyp27b1) and 24-OHase (Cyp24a1) expression. (A,B) mRNA and protein expression of Cyp27b1 in HK-2 cells after incubation in N, HP (4 mM), HNa (170 mM), EGTA, HP + EGTA and HNa + EGTA for 24 hours. (C,D) mRNA and protein expression of Cyp24a1 in HK-2 cells after incubation in N, HP (4 mM), HNa (170 mM), EGTA, HP + EGTA and HNa + EGTA for 24 hours. [a], versus N, P<0.05; [b], versus HP, P<0.05; [c], versus HNa, P<0.05. HK-2, human proximal tubule epithelial cell; N, normal medium; HP, high phosphate; HNa, high sodium; EGTA, ethylene glycol tetra acetic acid; HP + EGTA, high phosphate + ethylene glycol tetra acetic acid; HNa + EGTA, high sodium + ethylene glycol tetra acetic acid.

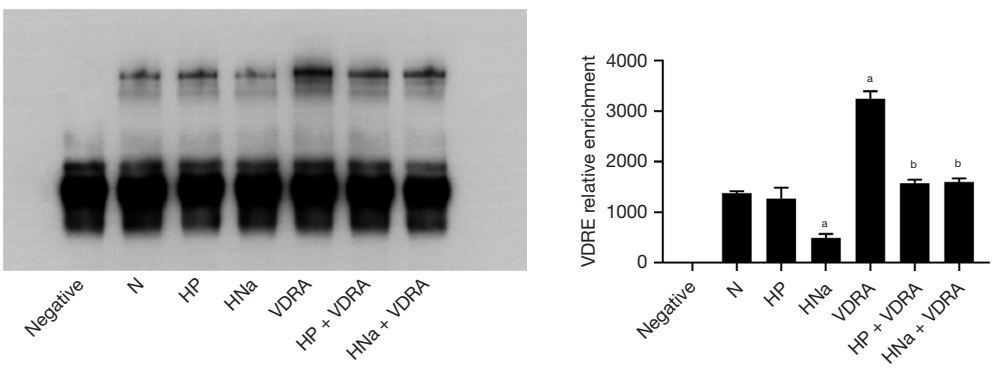

Figure 9 High sodium reduced, whereas VDRA promoted, the binding ability of VDR/RXRα to the VDRE of target gene Cyp24a1. [a], versus N, P<0.05; [b], versus VDRA, P<0.05. VDRA, vitamin D receptor activator; VDR/RXRα, vitamin D receptor/retinoid X receptor α; VDRE, vitamin D response element.

24-OHase was significantly higher than in the high sodium intervention group and higher than in the high phosphate group, indicating the predominant roles of sodium in lowering the expression of 1α-OHase and 24-OHase. These results suggest that high sodium has significant effects in reducing 1α-OHase and 24-OHase, which is mainly mediated by Npt2a and NHE3.

Ouabain, a sodium-K-ATPase inhibitor that can increase intracellular sodium, can affect various cellular biological functions. For example, studies found that 25/50/100 nM ouabain could reduce proliferation and viability and induce apoptosis of human lymphoma cells in a dose-

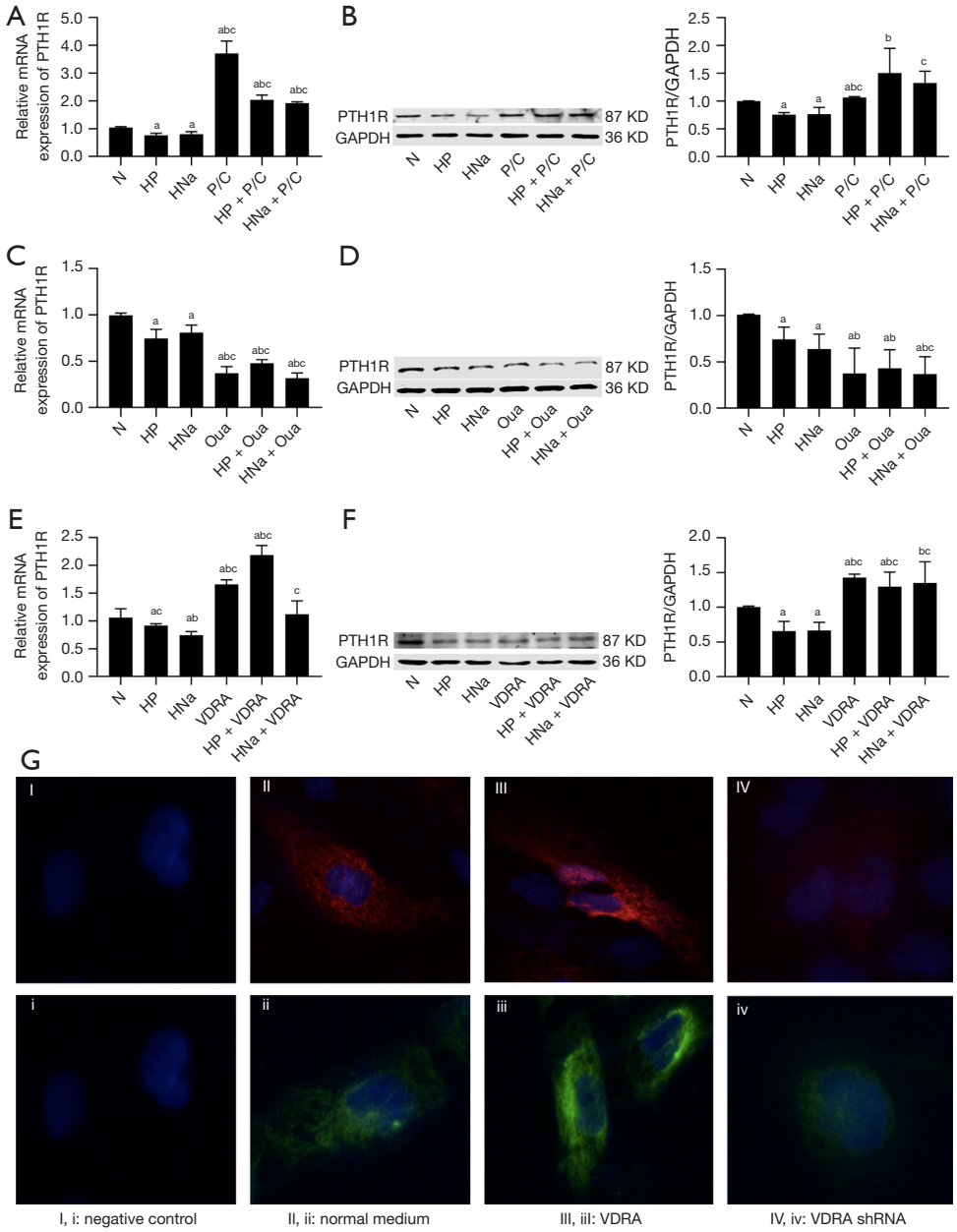

Figure 10 Effects of high sodium, PFA and cariporide, ouabain, and VDRA on the expression of PTH1R. (A,B) mRNA and protein expression of PTH1R in HK-2 cells after incubation in N, HP (4 mM), HNa (170 mM), P/C, HP + P/C and HNa + P/C for 24 hours. (C,D) mRNA and protein expression of PTH1R in HK-2 cells after incubation in N, HP (4 mM), HNa (170 mM), Oua, HP + Oua and HNa + Oua for 24 hours. (E,F) mRNA and protein expression of PTH1R in HK-2 cells after incubation in N, HP (4 mM), HNa (170 mM), VDRA, HP + VDRA and HNa + VDRA for 24 hours. (G) Immunofluorescence expression of PTH1R in HK-2 cells after incubation in the negative control, N, VDRA, and VDR shRNA for 24 hours (×400). Blue, 4',6-diamidino-2-phenylindole; Green, vitamin D receptor; Red, parathyroid receptor 1. [a], versus N, P<0.05; [b], versus HP, P<0.05; [c], versus HNa, P<0.05. PFA, phosphonoformic acid trisodium salt hexahydrate; HK-2, human proximal tubule epithelial cell; PTH1R, parathyroid receptor 1; N, normal medium; HP, high phosphate; HNa, high sodium; P/C, phosphonoformic acid trisodium salt hexahydrate + cariporide; HP + P/C, high phosphate + phosphonoformic acid trisodium salt hexahydrate + cariporide; HNa + P/C, high sodium + phosphonoformic acid trisodium salt hexahydrate + cariporide; Oua, ouabain; VDRA, vitamin D receptor activator; HP + VDRA, high phosphate + vitamin D receptor activator; HNa + VDRA, high sodium + vitamin D receptor activator; VDR shRNA, vitamin D receptor small hairpin RNA.

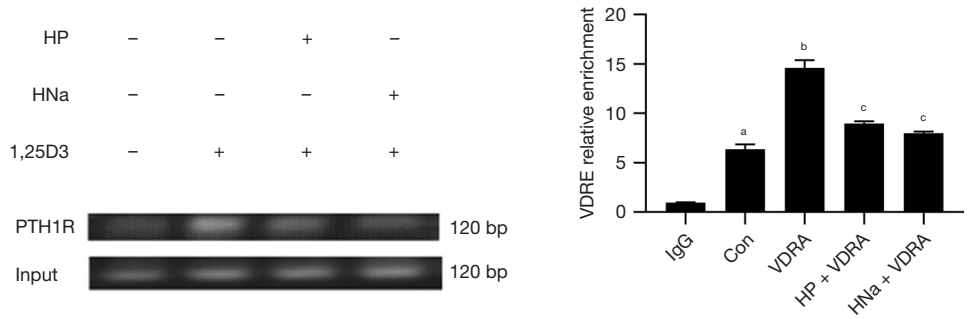

Figure 11 The recruitment of VDR/RXRα to the VDRE of PTH1R promoter. –, without intervention; +, with intervention; [a], versus IgG, P<0.05; [b], versus N, P<0.05; [c], versus VDRA, P<0.05. N, normal medium; VDR/RXRα, vitamin D receptor/retinoid X receptor α; VDRE, vitamin D response element; PTH1R, parathyroid receptor 1.

dependent way (25), while 3 nM ouabain could induce transdifferentiation of renal epithelial cells in patients with polycystic kidney disease without affecting normal renal epithelial cells (26). Therefore, the intervention of 10 nM ouabain in our study could increase the intracellular sodium concentration without affecting the biological processes, such as apoptosis and transdifferentiation. Furthermore, the results of ouabain intervention further demonstrated that the increase of intracellular sodium could reduce the expression of 1α-OHase and 24-OHase, thereby reducing the synthesis of $1,25(OH)_2D_3$.

In our study, KEGG enrichment analysis of DEGs revealed that high sodium/high phosphate intervention could activate the calcium signaling pathway. We envisage two main ways to increase intracellular calcium: one is the influx of extracellular calcium, and the other is th e release of calcium from intracellular calcium stores. Our results provided evidence that high sodium/high phosphate could promote extracellular calcium entry into HK-2 cells, then activate the calcium signaling pathway, thereby affecting the expression of vitamin D metabolism-related enzymes. The transepithelial voltage-dependent L-type calcium channels (27) and the transient receptor potential channel 1 (28) have been observed in the apical membrane of proximal tubule cells. They are considered to contribute to calcium-mediated intracellular signaling (29). As to the possible regulatory mechanisms of increased intracellular Ca^{2+} on 1α-OHase and 24-OHase, it was found that 1α-OHase activity in HKC-8 cells was sensitive to the concentration of calcium, treatment with medium containing high levels of calcium significantly inhibited $1,25\text{-}(OH)_2D_3$ production (30). The *in vitro* experiments indicated that both 1α-OHase and 24-OHase show similar responses to changes in calcium concentration. It suggested that high extracellular Ca^{2+} might inhibit the expression of 1α-OHase and 24-OHase probably by increasing intracellular Ca^{2+}. It also reported that at high Ca^{2+} concentrations, the calcium sensing receptor (CaSR) mediated a posttranscriptional mechanism, most probably 1α-OHase protein breakdown, dependent upon a mechanism that links the CaSR to phosphorylation of CaSR residue T888 via protein kinase C α (PKCα) and to an ERK1/2-dependent pathway, presumably downstream of CaSRT888 phosphorylation (31,32). As to the mechanisms of how the high sodium/phosphate intervention increased the intracellular calcium, it was also found that increases in intracellular sodium were paralleled by elevations in intracellular calcium through the reversible Na^+/Ca^{2+} exchanger, leading to the activation of SIK1 (Thr-322 phosphorylation) by a calcium calmodulin-dependent kinase (33). The possible mechanisms need further exploration.

We further studied the effects of high sodium and high phosphate intervention on the phosphate-regulating hormone in proximal tubule epithelial cells. The physiological effects of PTH are mediated by its specific membrane receptor PTH1R, which is widely distributed in many organs such as the kidney, heart, and bones. Our previous research found that in the early stage of kidney disease, renal PTH1R was down-regulated and worsened with the progression of renal damage (34). Massry *et al.* also found a decline in PTH1R in organs such as the liver and heart, which are not the specific target organs of PTH in CKD rats (35), indicating that a PTH1R decrease is a common phenomenon in CKD.

In addition to CKD, Katsumata *et al.* found that PTH1R

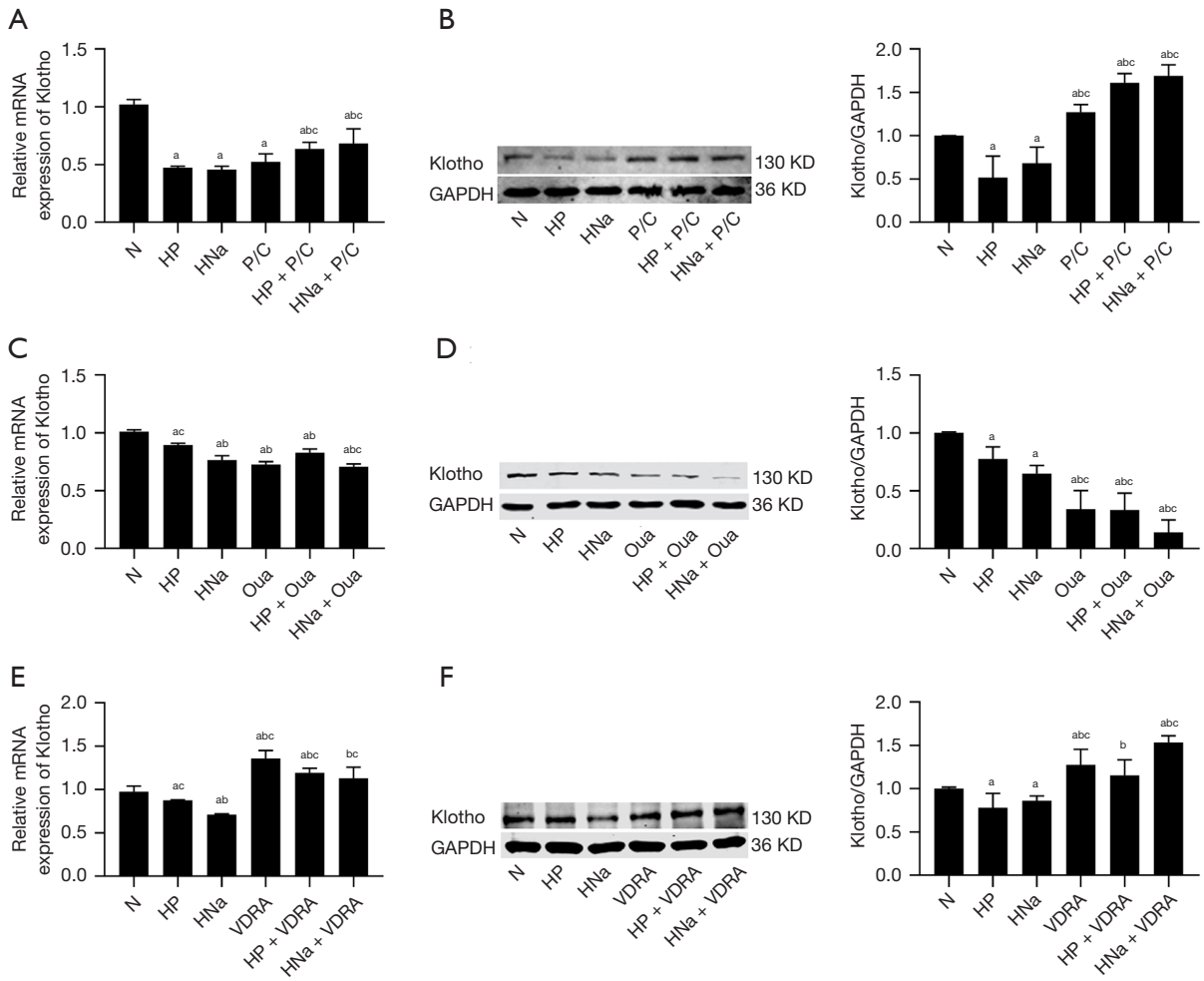

Figure 12 Effects of high sodium, PFA and cariporide, ouabain and VDRA on the expressions of Klotho. (A,B) mRNA and protein expression of Klotho in HK-2 cells after incubation in N, HP (4 mM), HNa (170 mM), P/C, HP + P/C and HNa + P/C for 24 hours. (C,D) mRNA and protein expression of Klotho in HK-2 cells after incubation in N, HP (4 mM), HNa (170 mM), Oua, HP + Oua and HNa + Oua for 24 hours. (E,F) mRNA and protein expression of Klotho in HK-2 cells after incubation in N, HP (4 mM), HNa (170 mM), VDRA, HP + VDRA and HNa + VDRA for 24 hours. [a], versus N, P<0.05; [b], versus HP, P<0.05; [c], versus HNa, P<0.05. PFA, phosphonoformic acid trisodium salt hexahydrate; HK-2, human proximal tubule epithelial cell; N, normal medium; HP, high phosphate; HNa, high sodium; P/C, phosphonoformic acid trisodium salt hexahydrate + cariporide; HP + P/C, high phosphate + phosphonoformic acid trisodium salt hexahydrate + cariporide; HNa + P/C, high sodium + phosphonoformic acid trisodium salt hexahydrate + cariporide; Oua, ouabain; VDRA, vitamin D receptor activator; HP + VDRA, high phosphate + vitamin D receptor activator; HNa + VDRA, high sodium + vitamin D receptor activator.

expression in the kidney of normal rats decreased after 21 days of a high-phosphate diet (36). The high- phosphate intervention in our *in vitro* experiments also decreased the expression of PTH1R. Interestingly, in addition to high phosphate, high sodium intervention could also reduce the expression of PTH1R in proximal tubule epithelial cells, which has not been previously reported. Our previous studies confirmed that when renal function declined, PTH1R expression in patients' lymphocytes was significantly down-regulated, and active vitamin D3 could increase PTH1R expression (37), which suggests an interaction between PTH1R and active vitamin D3.

In addition to the main site of $1,25(OH)_2D_3$ synthesis and metabolism, proximal tubule epithelial cells are also the

target cells of $1,25(OH)_2D_3$, and the effects of $1,25(OH)_2D_3$ are mainly carried out by the nuclear receptor VDR, which is abundant in the brush border of proximal tubule epithelial cells. The genomic mechanism of $1,25(OH)_2D_3$ action involves the direct binding of the $1,25(OH)_2D_3$ activated vitamin D receptor/retinoic X receptor (VDR/RXR) heterodimeric complex to specific DNA sequences (38). We and others have found that VDRE exists in the promoter of the *PTH1R* gene in proximal tubular epithelial cells (39,40). In our study, VDRA could significantly promote the binding ability of VDR/RXRα and the VDRE of the target gene *PTH1R*, and increase the expression of *PTH1R*, indicating that high sodium and high phosphate can reduce *PTH1R* expression in proximal renal tubules by inhibiting the synthesis and local gene regulation of $1,25(OH)_2D_3$. As we know, PTH needs to interact with its receptor *PTH1R*, acting on the sodium phosphate co-transporters on the proximal tubule, inhibiting the reabsorption of phosphate, thereby promoting the excretion of phosphate. We speculate that the down-regulation of *PTH1R* in proximal tubular epithelial cells may reduce phosphate excretion, thus stimulating PTH synthesis and secretion in the parathyroid glands. In addition, the decreased *PTH1R* levels might inhibit the effects of PTH on renal $1,25(OH)_2D_3$ synthesis, reduce calcium absorption in the intestines, and further promote PTH secretion. Thus, a long-term high sodium diet may induce secondary hyperparathyroidism by reducing *PTH1R* expression, which could be confirmed in our ongoing animal studies.

Similarly, Forster *et al.* reported that $1,25(OH)_2D_3$ could regulate Klotho expression through VDRE, which was found in the promoter of the Klotho gene of human renal tubular epithelial cells (39). Our *in vitro* studies revealed that high sodium/high phosphate significantly reduces the expression of Klotho by inhibiting the synthesis of active $1,25(OH)_2D_3$. Fibroblast growth factor receptor 1 (FGFR1) is a transmembrane protein and member of the FGFR family. FGF23, a bone-derived phosphotropic hormone, mainly regulates kidney phosphate and vitamin D metabolism via the FGFR1/α-Klotho complex (41). As an important cofactor of the phosphate-regulating hormone FGF23, the decrease of Klotho may cause local resistance of FGF23 and further stimulate FGF23 secretion. Furthermore, it is known that $1,25(OH)_2D_3$ and FGF23 can inhibit the secretion of PTH under normal circumstances. Since high sodium/high phosphate could reduce the synthesis and function of $1,25(OH)_2D_3$ and Klotho in the proximal tubules, PTH would continuously be secreted due to the loss of the inhibitory effect of active vitamin D3 and FGF23/Klotho, which would promote the development of secondary hyperparathyroidism.

Conclusions

In conclusion, high sodium could reduce the expression of PTH1R and Klotho by decreasing the synthesis of active vitamin D, and affecting the gene regulation of 1,25(OH)2D3/VDR in the proximal tubules. Our data suggest the influence of a high-sodium diet on mineral metabolism and the core role of vitamin D in kidney mineral metabolism, which is particularly relevant given the high-sodium modern diet.

Acknowledgments

We thank Shanghai Engineering Research Center of AI Assisted Clinical Service for Aging-Associated Diseases (19DZ2251700) for technical support. Our manuscript has been presented as a poster at the American Society of Nephrology (ASN) Kidney Week 2021 (ePoster number: PO0515).

Funding: This work was supported by grants from National Key R&D Program of China (No. 2020YFC2005000), Key Project of National Natural Science Foundation of China (No. 81730017), Shanghai Medical Leading Talents Fund (No. 2019LJ03), Innovation action plan project of Shanghai Science and Technology Commission (Nos. 17411950700, 20Y11904500 and 21ZR1411100).

Footnote

Reporting Checklist: The authors have completed the MDAR reporting checklist. Available at https://atm.amegroups.com/article/view/10.21037/atm-21-5910/rc

Data Sharing Statement: Available at https://atm.amegroups.com/article/view/10.21037/atm-21-5910/dss

Conflicts of Interest: All authors have completed the ICMJE uniform disclosure form (available at https://atm.amegroups.com/article/view/10.21037/atm-21-5910/coif). The authors have no conflicts of interest to declare.

Ethical Statement: The authors are accountable for all aspects of the work, including ensuring that any questions related to the accuracy or integrity of any part of the work

have been appropriately investigated and resolved.

References

1. Da J, Xie X, Wolf M, et al. Serum Phosphorus and Progression of CKD and Mortality: A Meta-analysis of Cohort Studies. Am J Kidney Dis 2015;66:258-65.
2. Kestenbaum B, Sampson JN, Rudser KD, et al. Serum phosphate levels and mortality risk among people with chronic kidney disease. J Am Soc Nephrol 2005;16:520-8.
3. Tonelli M, Sacks F, Pfeffer M, et al. Relation between serum phosphate level and cardiovascular event rate in people with coronary disease. Circulation 2005;112:2627-33.
4. Yoo KD, Kang S, Choi Y, et al. Sex, Age, and the Association of Serum Phosphorus With All-Cause Mortality in Adults With Normal Kidney Function. Am J Kidney Dis 2016;67:79-88.
5. Komaba H, Fukagawa M. Phosphate-a poison for humans? Kidney Int 2016;90:753-63.
6. Ritter CS, Slatopolsky E. Phosphate Toxicity in CKD: The Killer among Us. Clin J Am Soc Nephrol 2016;11:1088-100.
7. Ide N, Ye R, Courbebaisse M, et al. In vivo evidence for an interplay of FGF23/Klotho/PTH axis on the phosphate handling in renal proximal tubules. Am J Physiol Renal Physiol 2018;315:F1261-70.
8. Clerin V, Saito H, Filipski KJ, et al. Selective pharmacological inhibition of the sodium-dependent phosphate cotransporter NPT2a promotes phosphate excretion. J Clin Invest 2020;130:6510-22.
9. Beck L, Karaplis AC, Amizuka N, et al. Targeted inactivation of Npt2 in mice leads to severe renal phosphate wasting, hypercalciuria, and skeletal abnormalities. Proc Natl Acad Sci U S A 1998;95:5372-7.
10. Block GA, Rosenbaum DP, Leonsson-Zachrisson M, et al. Effect of Tenapanor on Interdialytic Weight Gain in Patients on Hemodialysis. Clin J Am Soc Nephrol 2016;11:1597-605.
11. Labonté ED, Carreras CW, Leadbetter MR, et al. Gastrointestinal Inhibition of Sodium-Hydrogen Exchanger 3 Reduces Phosphorus Absorption and Protects against Vascular Calcification in CKD. J Am Soc Nephrol 2015;26:1138-49.
12. Goulding A, McIntosh J. Effects of NaCl on calcium balance, parathyroid function and hydroxyproline excretion in prednisolone-treated rats consuming low calcium diet. J Nutr 1986;116:1037-44.
13. Yang L, Leong PK, Chen JO, et al. Acute hypertension provokes internalization of proximal tubule NHE3 without inhibition of transport activity. Am J Physiol Renal Physiol 2002;282:F730-40.
14. Good DW, George T, Watts BA 3rd. High sodium intake increases HCO(3)- absorption in medullary thick ascending limb through adaptations in basolateral and apical Na+/H+ exchangers. Am J Physiol Renal Physiol 2011;301:F334-43.
15. Yang LE, Maunsbach AB, Leong PK, et al. Differential traffic of proximal tubule Na+ transporters during hypertension or PTH: NHE3 to base of microvilli vs. NaPi2 to endosomes. Am J Physiol Renal Physiol 2004;287:F896-906.
16. Bai XY, Miao D, Goltzman D, et al. The autosomal dominant hypophosphatemic rickets R176Q mutation in fibroblast growth factor 23 resists proteolytic cleavage and enhances in vivo biological potency. J Biol Chem 2003;278:9843-9.
17. Yoshikawa R, Yamamoto H, Nakahashi O, et al. The age-related changes of dietary phosphate responsiveness in plasma 1,25-dihydroxyvitamin D levels and renal Cyp27b1 and Cyp24a1 gene expression is associated with renal α-Klotho gene expression in mice. J Clin Biochem Nutr 2018;62:68-74.
18. Condamine L, Menaa C, Vrtovsnik F, et al. Local action of phosphate depletion and insulin-like growth factor 1 on in vitro production of 1,25-dihydroxyvitamin D by cultured mammalian kidney cells. J Clin Invest 1994;94:1673-9.
19. Slominski AT, Kim TK, Li W, et al. Detection of novel CYP11A1-derived secosteroids in the human epidermis and serum and pig adrenal gland. Sci Rep 2015;5:14875.
20. Bailey D, Veljkovic K, Yazdanpanah M, et al. Analytical measurement and clinical relevance of vitamin D(3) C3-epimer. Clin Biochem 2013;46:190-6.
21. Portale AA, Halloran BP, Morris RC Jr. Physiologic regulation of the serum concentration of 1,25-dihydroxyvitamin D by phosphorus in normal men. J

Clin Invest 1989;83:1494-9.
22. Portale AA, Halloran BP, Morris RC Jr. Dietary intake of phosphorus modulates the circadian rhythm in serum concentration of phosphorus. Implications for the renal production of 1,25-dihydroxyvitamin D. J Clin Invest 1987;80:1147-54.
23. Antoniucci DM, Yamashita T, Portale AA. Dietary phosphorus regulates serum fibroblast growth factor-23 concentrations in healthy men. J Clin Endocrinol Metab 2006;91:3144-9.
24. van der Wijst J, Tutakhel OAZ, Bos C, et al. Effects of a high-sodium/low-potassium diet on renal calcium, magnesium, and phosphate handling. Am J Physiol Renal Physiol 2018;315:F110-22.
25. Meng L, Wen Y, Zhou M, et al. Ouabain induces apoptosis and autophagy in Burkitt's lymphoma Raji cells. Biomed Pharmacother 2016;84:1841-8.
26. Venugopal J, McDermott J, Sanchez G, et al. Ouabain promotes partial epithelial to mesenchymal transition (EMT) changes in human autosomal dominant polycystic kidney disease (ADPKD) cells. Exp Cell Res 2017;355:142-52.
27. Zhang MI, O'Neil RG. Regulated calcium channel in apical membranes renal proximal tubule cells. Am J Physiol 1996;271:C1757-64.
28. Goel M, Sinkins WG, Zuo CD, et al. Identification and localization of TRPC channels in the rat kidney. Am J Physiol Renal Physiol 2006;290:F1241-52.
29. Lipscombe D, Helton TD, Xu W. L-type calcium channels: the low down. J Neurophysiol 2004;92:2633-41.
30. Bland R, Walker EA, Hughes SV, et al. Constitutive expression of 25-hydroxyvitamin D3-1alpha-hydroxylase in a transformed human proximal tubule cell line: evidence for direct regulation of vitamin D metabolism by calcium. Endocrinology 1999;140:2027-34.
31. Huang A, Binmahfouz L, Hancock DP, et al. Calcium-Sensing Receptors Control CYP27B1-Luciferase Expression: Transcriptional and Posttranscriptional Mechanisms. J Endocr Soc 2021;5:bvab057.
32. McCormick WD, Atkinson-Dell R, Campion KL, et al. Increased receptor stimulation elicits differential calcium-sensing receptor(T888) dephosphorylation. J Biol Chem 2010;285:14170-7.
33. Sjöström M, Stenström K, Eneling K, et al. SIK1 is part of a cell sodium-sensing network that regulates active sodium transport through a calcium-dependent process. Proc Natl Acad Sci U S A 2007;104:16922-7.
34. Chen J, Zhang J, Lin S. Down-regulation of PTH/PTHrP receptor in the kidney of patients with renal impairment. Chin Med J (Engl) 1998;111:24-7.
35. Massry SG, Smogorzewski M. Mechanisms through which parathyroid hormone mediates its deleterious effects on organ function in uremia. Semin Nephrol 1994;14:219-31.
36. Katsumata S, Masuyama R, Uehara M, et al. Decreased mRNA expression of the PTH/PTHrP receptor and type II sodium-dependent phosphate transporter in the kidney of rats fed a high phosphorus diet accompanied with a decrease in serum calcium concentration. Biosci Biotechnol Biochem 2004;68:2484-9.
37. Chen J, Cu Y, Zhang J, et al. Effects of nifedipine and calcitriol on the PTH/PTHrP receptor mRNA expression in uremic patients. Chin J Nephrol 2000;16:4.
38. Christakos S, Dhawan P, Verstuyf A, et al. Vitamin D: Metabolism, Molecular Mechanism of Action, and Pleiotropic Effects. Physiol Rev 2016;96:365-408.
39. Forster RE, Jurutka PW, Hsieh JC, et al. Vitamin D receptor controls expression of the anti-aging klotho gene in mouse and human renal cells. Biochem Biophys Res Commun 2011;414:557-62.
40. Ritter CS, Zhang S, Delmez J, et al. Differential expression and regulation of Klotho by paricalcitol in the kidney, parathyroid, and aorta of uremic rats. Kidney Int 2015;87:1141-52.
41. Takashi Y, Fukumoto S. FGF23 beyond Phosphotropic Hormone. Trends Endocrinol Metab 2018;29:755-67.vv

Cite this article as: Gu J, Shi J, Chen X, Mao J, You H, Chen J. High sodium reduced the expression of PTH1R and Klotho by inhibiting $1,25(OH)_2D_3$ synthesis in cultured proximal tubule epithelial cells. Ann Transl Med 2022;10(9):506. doi: 10.21037/atm-21-5910

Supplementary

Table S1 Recreation system for mRNA reverse transcription

Reagent	Volume (μL)
5xReaction Buffer	4.0
10mM dNTPmix	1.0
Recombinant Rnasin (40 Units/μL)	0.3
M-MLV (200 Units/μL)	0.8
RNase-free ddH_2O	3.9
Count	10

Table S2 Recreation system for PCR

Reagent	Volume (μL)
Real-time quantitative PCR Premix mixture (2X)	10
Upstream primer (2 μM)	2
Downstream primer (2 μM)	2
DNA samples are pending	1
PCR water	5
Total volume	20

https://dx.doi.org/10.21037/atm-21-5910